^{1}H NMR Structural Characterization of a Nonmitogenic, Vasodilatory, Ischemia-Protector and Neuromodulatory Acidic Fibroblast Growth Factor†

Rosa M. Lozano,‡,§ Antonio Pineda-Lucena,‡,§ Carlos Gonzalez,|| M. Ángeles Jiménez,|| Pedro Cuevas,⊥ Mariano Redondo-Horcajo,§ Jesús M. Sanz,§ Manuel Rico,|| and Guillermo Giménez-Gallego*,§

Centro de Investigaciones Biológicas (CSIC), Velázquez 144, 28006 Madrid, Spain, Instituto de Estructura de la Materia (CSIC), Serrano 119, 28006 Madrid, Spain, and Servicio de Histología, Hospital Universitario Ramón y Cajal, 28034 Madrid, Spain

Received November 4, 1999; Revised Manuscript Received February 9, 2000

ABSTRACT: A shortened genetically engineered form of acidic fibroblast growth factor (aFGF), that includes amino acids 28−154 of the full-length sequence (154 residues) plus Met in substitution of Leu27, does not induce cell division even though it is recognized by the cell membrane receptor, triggers the early mitogenic events, and retains the neuromodulatory, vasoactive, and cardio- and neuroprotective properties of the native full-length molecule. Taken together, these properties make this truncated aFGF a promising compound in the treatment of a wide assortment of neurological and cardiovascular pathologies where aFGF mitogenic activity is dispensable. Differences in biological activities between the shortened aFGF and the wild-type form have been attributed to lack of stability, and to the specific amino acid sequence missing at the N-terminus. Here we show that this shortened aFGF form has a three-dimensional structure even more stable than the wild-type protein at the mitogenic assay conditions; that this structure is similar to that of the wild type except at site 1 of interaction with the cell membrane receptor; that its lack of mitogenic activity cannot be attributed to the specific missing sequence; and that the vasodilatory activity of aFGF seems impaired by alterations of the three-dimensional structure of site 2 of interaction with the cell membrane receptor.

Acidic fibroblast growth factor (aFGF)[1] was the first member to be described of a family of 19 (up to now) closely related proteins. aFGF and the subsequently discovered basic fibroblast growth factor (bFGF) are considered prototypes for the whole family (*1*−*3*). Both polypeptides are very powerful and broad-spectrum mitogens. Actually, all the cells of mesodermal and neuroectodermal origin studied thus far are stimulated to divide by either aFGF or bFGF when tested in vitro (*4*, *5*).

Mitogenic induction by FGFs begins with the interaction of these proteins, at the cell surface, with specific transmembrane tyrosine kinases (*6*). The FGF residues interacting with these tyrosine kinases cluster in two separate patches of the three-dimensional structure of FGFs: recognition site-1 (RS1) that includes residues belonging to β-strands 1, 2, and 12 and β-strand connections 1−2, 3−4, and 8−9; and recognition site-2 (RS2) constituted by residues of the connection of β-strand 9 with 10 (*7*−*12*). Activation of these receptors by FGFs requires the presence of heparin, a compound toward which they show a characteristic high affinity and that can be substituted by *myo*-inositol hexasulfate (MIHS; *4*, *5*, *10*, *13*). Binding of FGFs to the cell-surface receptors triggers autophosphorylation of at least seven different tyrosine residues (*14*) and activates at least two different signaling cascades that converge to a common signaling molecule, Raf-1, an activator of the downstream MAPK signaling cascade (*15*). Recognition of FGF by the cell-surface receptors also causes an almost immediate enhancement of intracellular Ca^{2+}, c-*fos*, c-*jun*, and c-*myc* mRNA levels, even in the presence of cycloheximide (*16*−*19*). In addition, it has also been shown that externally supplied FGF is translocated to the nucleus, a process revealed to be absolutely necessary for the completion of mitogenesis (*20*, *21*).

Purification of aFGF from different tissues and animals has yielded forms of varying lengths, all of which are probably derived from the full-length 154-amino acid polypeptide by proteolysis of the N-terminus during the purification (*22*−*28*). The three-dimensional structures of the full-length and shortened forms of the protein from either X-ray diffraction or two-dimensional ^{1}H NMR data show

† R.M.L. was a recipient of a Contrato de Reincorporación from the Spanish Ministerio de Educación y Ciencia. This work was partially funded by the Dirección General de Investigación Científica y Técnica and Fundación Futuro.

* Corresponding author.
‡ These authors contributed equally to this project.
§ Centro de Investigaciones Biológicas (CSIC).
|| Instituto de Estructura de la Materia (CSIC).
⊥ Servicio de Histología, Hospital Universitario Ramón y Cajal.

[1] Abbreviations: aFGF, acidic FGF; $aFGF^{23-154}$, $aFGF^{23-154}$ spanning residues 23−154 of the full-length aFGF sequence (154 residues); $aFGF^{27-154}$, aFGF spanning residues 27−154 of the full-length aFGF sequence; $aFGF^{4Ala}$, aFGF spanning residues 23−154 of the full-length aFGF sequence with residues 23−26 substituted by four alanines; bFGF, basic FGF; COSY, homonuclear correlated spectroscopy; FGF, fibroblast growth factor; MIHS, *myo*-inositol hexasulfate; NMR, nuclear magnetic resonance; NOE, nuclear Overhauser effect; NOESY, nuclear Overhauser enhancement spectroscopy; RMSD, root-mean-square deviation; RS1, FGF site-1 for recognition of its cell membrane tyrosine kinase receptor; RS2, FGF site-2 for recognition of its cell membrane tyrosine kinase receptor; TOCSY, total correlation spectroscopy.

10.1021/bi992544n CCC: $19.00
Published on Web 04/06/2000

	23							30						
$aFGF^{23-154}$	K	K	P	K	L	L	Y	C	S	N	G	G	H	F	L
$aFGF^{27-154}$					M	L	Y	C	S	N	G	G	H	F	L
$aFGF^{4Ala}$	A	A	A	A	L	L	Y	C	S	N	G	G	H	F	L

FIGURE 1: Primary structure of the amino-terminus for $aFGF^{23-154}$, $aFGF^{27-154}$, and $aFGF^{4Ala}$. Amino acids are represented by single-letter code. Residues are numbered (top line) according to the primary structure of the full-length aFGF (154 residues; *25*). Residues at positions 23−27 are identical in $aFGF^{23-27}$ and the native full-length sequence.

that the first 23 N-terminal residues of aFGF are disordered (*8*, *10*, *11*, *29*). The lack of defined structure in this region of the protein is consistent with a proteolytic degradation during the purification from animal tissues (*28*, *30*−*32*).

No significant differences in stability and biological properties have been detected between the different truncated forms of aFGF, including the one beginning at Lys23 ($aFGF^{23-154}$; *25*, *10*). The 15 amino-terminal residues of this last aFGF form appear in Figure 1. Nevertheless, elimination of the four subsequent residues, Lys-Lys-Pro-Lys- (residues 23−26), plus the highly conservative substitution of Leu27 by Met (*33*) yields $aFGF^{27-154}$ (Figure 1), which has the characteristic high affinity for heparin and ability to trigger early mitogenic events such as the intracellular receptor-mediated tyrosine phosphorylation and c-*fos* expression of mitogenically active FGFs, but fails to induce DNA synthesis and cell proliferation (*34*). Alignment of FGFs and site-directed mutagenesis studies show that this family of proteins accepts a wide variety of amino acids at position 27 without apparent alteration in specific activity (*2*, *9*). Thus, failure of $aFGF^{27-154}$ in inducing cell division has been attributed to the specific absence of the stretch Lys-Lys-Pro-Lys. On the basis of its similarity with the nuclear translocation sequences of some nuclear proteins (*35*, *36*), it was proposed that this 23−26 residue stretch could be responsible, at least in part, for the translocation of the protein to the nucleus (*34*, *37*). Later on, it was shown that, effectively, in contrast to the mitogenic forms of aFGF, $aFGF^{27-154}$ does not translocate to the nucleus, but remains in the cytoplasmic fraction (*38*). Furthermore, attachment of the homologous nuclear translocation sequence from yeast histone 2B at the amino terminus of $aFGF^{27-154}$ restores full mitogenic activity (*34*). Finally, it has been shown that cell membrane-permeable peptides containing the Lys-Lys-Pro-Lys sequence can stimulate DNA synthesis in a relatively wide assortment of cell lines, in a FGF receptor-independent manner (*39*, *40*), which suggests an additional and more direct involvement of this sequence in aFGF-induced mitogenesis. Luo et al. (*41*) have shown, on the basis of studies on denaturation rates at 85 °C and resistance to trypsin digestion, that $aFGF^{27-154}$ three-dimensional structure is less stable than the longer forms of the protein.

Endocrine-like activities not involving mitogenesis have also been ascribed to FGFs (*5*). Thus, we have shown that FGFs are very powerful vasodilators, the effect mediated by the activation of the ATP-sensitive K^+ channels and the constitutive endothelial nitric oxide synthetase (*42*). In addition, we have shown that FGFs are very efficient protectors of brain and heart tissues against the effects of transient ischemia, a protection that does not require cell division (*43*, *44*). Finally, we have also shown that FGFs are powerful short-term depressors of the locomotor, exploratory, and stereotypic behavior of rats, effects not accompanied by changes either in the arterial blood pressure or in body temperature, but somehow involving an enhanced synthesis of nitrogen oxide (*45*). In all these cases, we have shown that $aFGF^{27-154}$ perfectly substitutes the normal mitogenic forms of FGFs, which obviously implies that the early events triggered by FGF binding to the cell-surface receptors are sufficient for sustaining them (*42*−*45*). The absence of any appreciable sign of mitogenesis when $aFGF^{27-154}$ is applied in vivo (*43*) makes this form an interesting candidate for therapeutic developments not requiring aFGF mitogenic activity, since it may allow the circumvention of the secondary effects derived from the application of a broad-spectrum mitogen to an organism. Given the potential pharmacological interest of $aFGF^{27-154}$ characterization, at high resolution, of the structural basis of its biological properties was undertaken. We found that $aFGF^{27-154}$ shows a well-defined and stable structure at physiological temperatures; that although the topology of its structure is that of the wild-type protein some readjustments caused by the shortening of β-strand 1 modify RS1; that shielding of Cys131 to the solvent could account for the enhanced stability of $aFGF^{27-154}$ with respect to the wild-type protein under mitogenic assay conditions; that the sequence Lys23-Lys24-Pro25-Lys26 is not a necessary component for aFGF to show a nearly full mitogenic activity, as it can be substituted by the sequence Ala-Ala-Ala-Ala; and that alteration of the three-dimensional structure of RS2 impairs the vasodilatory activity of aFGF.

MATERIALS AND METHODS

Reagents. Heparin−Sepharose was obtained from Pharmacia; nitrocellulose filters were from Millipore; culture plates were from Costar; bacteriological agar, yeast extract, and tryptone were from Gibco BRL; ITS+ culture supplement was from Collaborative Research Inc.; ethanolamine, MIHS, and Na-heparin (average molecular mass 3 kDa) were from Sigma; L-glutamine, Ham's F-12 medium, and DMEM were from Flow. Macrosep ultrafiltration cartridges (Omega type, low binding protein membrane, 3 kDa cutoff) were from Filtron Technology Corp. Distilled water filtered through a Milli-Q7 (Millipore) water purifier fitted with an Organex7 column (Millipore) was used in all solutions.

Protein Preparation. Residues are numbered according to their position in the primary structure of the 154 amino acid aFGF (*25*). Expression vector for $aFGF^{27-154}$ (pMG62) was constructed by eliminating the segment between the restriction enzymes *Nco*I and M*st*II in pFD34 (*46*) with the appropriate synthetic DNA fragment. Afterward the segment between restriction sites *Eco*RI and *Hin*dIII was cloned into the equivalent sites of pINIII-A3 vector (*47*). In the case of $aFGF^{4Ala}$, the fragment between *Nco*I and *Hin*dIII $aFGF^{27-154}$ in pMG62 was amplified by PCR with the appropriate primers to introduce at the N-terminus of $aFGF^{27-154}$ the sequence Ala-Ala-Ala-Ala-. The amplified fragment was introduced subsequently in pINIII-A3 vector between restriction sites *Xba*I and *Hin*dIII to create the corresponding expression vector (pMG624A). Accuracy of the genes was checked by DNA sequencing. Protein expression was carried out in *Escherichia coli* AB1899 [lac^+] (*46*). The protein was prepared as described in Pineda-Lucena et al. (*10*), except that in the case of $aFGF^{27-154}$ and $aFGF^{4Ala}$, where the protein was not expressed as a fusion protein, chymotryptic digestion

was not required. Automatic N-terminal Edman degradation (Applied Biosystem 494) showed that aFGF$^{27-154}$, but not aFGF^{4Ala}, conserves the initiator Met residue. For the ^{1}H NMR studies, the protein was prepared and equilibrated against a solution of 2 mM MIHS as described (*10*). The appropriate amounts of ^2H_2O and 3-trimethylsilylpropionate, as chemical shift reference, were added at the preparation in a final step. The native state of the protein was routinely monitored during the preparation of the ^{1}H NMR sample by fluorescence spectroscopy (*46*, *10*).

Urea Denaturation. Equilibrium denaturation studies were carried out by measuring the dependence of the CD signal at 227 nm on the urea concentration, in the equipment and by the procedures previously described (*48*). The stability of the structure of the protein, in terms of a two-state transition (*49*), was estimated as $\Delta G_D^{H_2O} = \underline{m}[U]_{1/2}$, where $\underline{m}$ is the average cooperativity value describing the change in ΔG with the concentration of denaturant measured for the three species under study, and $[U]_{1/2}$ is the urea concentration at the midpoint of the transition. Use of $\underline{m}$ instead of the particular m in each case lowers the standard error for the calculation of $\Delta G_D^{H_2O}$ values (*50*).

NMR Spectroscopy. 2D NMR data were acquired in a Bruker AMX-600 spectrometer in the phase-sensitive mode using the time-proportional phase incrementation method (*51*). Water suppression was carried out either by selective presaturation placing the carrier on the solvent resonance or by including a WATERGATE module (*52*). Conventional pulse sequences were used for homonuclear correlated spectroscopy (COSY; *53*) and nuclear Overhauser enhancement spectroscopy (NOESY; *54*). The mixing time in the NOESY experiment was set to 150 ms. Data for total correlation spectroscopy (TOCSY; *55*) were acquired using the standard MLEV17 spin-locking sequence and 60 ms mixing time. The spectra of aFGF were recorded at 298 K. A spectral width of 9600 Hz in both dimensions was used. The size of the acquisition data matrix was 2048 × 512 words in t_2 and t_1, respectively, and zero-filling up to 4K in t_2 and 1K in t_1 was made prior to the Fourier transformation. Shifted sine-bell or squared sine-bell window functions, with the corresponding shift optimized for every spectrum, were used for resolution enhancement, and base line correction was applied in both dimensions.

Analysis of phase-sensitive 150 ms NOESY spectra for 1 mM solutions of the proteins was carried out with the program XEASY (*56*). The integration routines in the XEASY package were used to obtain the intensities of the NOE cross-peaks. These intensities were converted into upper distance bounds with the program CALIBA (*57*). The necessary scaling factors were chosen to reproduce the correct distance limits for proton pairs separated by fixed distances, e.g., HB2−HB3 distances, αCH−methyl in Val, etc. Cross-peaks which could not be integrated due to partial overlap were qualitatively classified as strong, medium, and weak, and assigned distance constraints of 3.0, 4.0, and 5.0 Å, respectively. For protons not stereospecifically assigned, and the methyl and aromatic protons, the usual pseudoatom corrections were applied.

The three-dimensional structures were calculated by restrained molecular dynamics using the program GROMOS (*58*). Three structures of the wild-type aFGF bound to MIHS (*10*) were used as starting point for the calculations. The necessary residues were either mutated or eliminated with the molecular modeling package SYBYL (Tripos Inc., St. Louis, MO). For the molecular dynamics calculations, the structures were brought from 300 to 1000 K in 5 ps and maintained there for an additional 40 ps. During this period of time, eight structures were sampled (each one for 5 ps) and then separately cooled to 600 K, maintained at this temperature for 5 ps, and then finally brought to 300 K, a temperature at which they were kept for an additional 5 ps. The last 2 ps of this trajectory was averaged, and the resulting structure was energy-minimized. The final number of conformers thus obtained was 24.

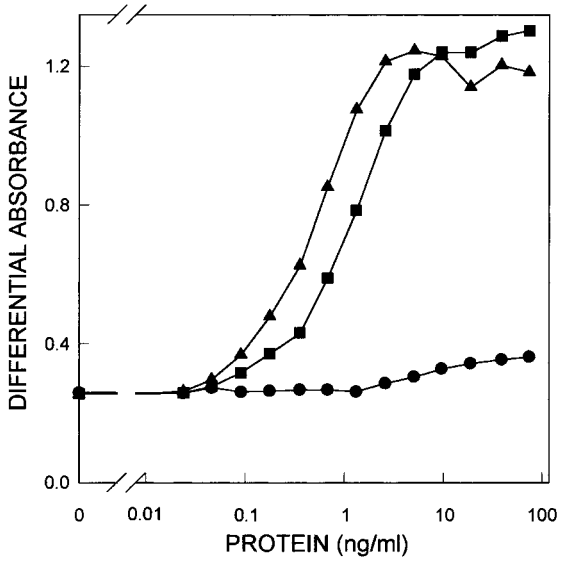

FIGURE 2: Mitogenic activity of aFGF$^{23-154}$ (▲), aFGF$^{27-154}$ (●), and aFGF^{4Ala} (■). Plots represent the stimulation of cell division by increasing concentrations of growth factor in the presence of 50 μg/mL heparin.

Proliferation Assays. Mitogenic activity was assayed as described by Ortega et al. (*59*). Cells were counted by measuring the total amount of crystal violet retained by cell nuclei by differential absorption (620 minus 690 nm; *46*, *59*). One mitogenic unit is the amount of FGF per milliliter that generates half-maximal stimulation as determined from full dose−response assays. The specific mitogenic activity is the number of stimulatory units per milligram of pure FGF.

RESULTS

Mitogenic Activity of aFGF$^{27-154}$ and aFGF^{4Ala}. Since FGF-driven mitogenesis requires its translocation to the nucleus, lack of mitogenic activity of aFGF$^{27-154}$ and failure to accumulate in this organelle have been first attributed to the loss of the potential nuclear localization sequence Lys-Lys-Pro-Lys. In addition, synthetic peptides containing this sequence seem able to trigger by themselves the synthesis of DNA (see the introduction). To ascertain a more precise picture of the role of this sequence, it was substituted by four alanines in aFGF$^{23-154}$ (aFGF^{4Ala}; Figure 1). As Figure 2 shows, the specific activity of aFGF^{4Ala} is quite close to that of the wild-type protein (1×10^6 vs 1.2×10^6 units/mg), while no appreciable activity was detectable in the case of aFGF$^{27-154}$ (consistent results obtained in three separate assays). Consequently, aFGF does not seem to require a nuclear localization consensus sequence at its N-terminus for mitogenic activity. Obviously the results of Figure 2 also

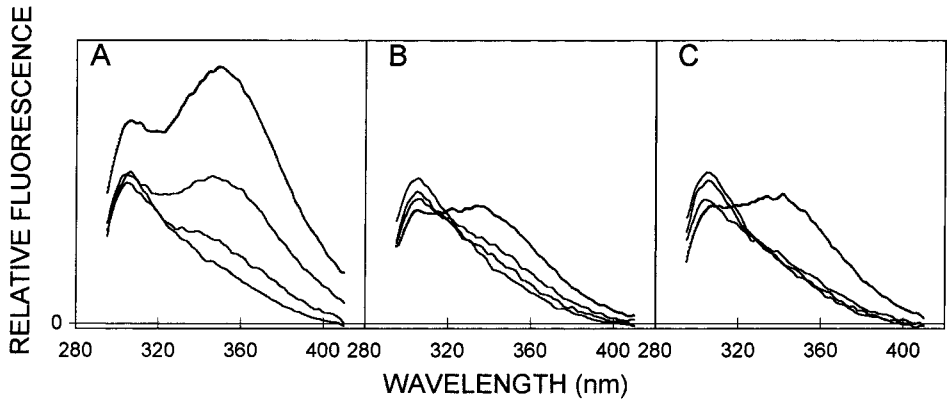

FIGURE 3: Progressive enhancement of the Trp fluorescence of aFGF$^{23-154}$ (A), aFGF$^{27-154}$ (B), and aFGF^{4Ala} (C) during 24 h in the cell incubator (5% CO_2 atmosphere; 310 K) in solutions with an ionic composition equivalent to the mitogenesis assay medium (Na-heparin, 50 μg/mL; NaCl, 90 mM; $CaCl_2$, 75 μM; $CuSO_4$, 0.25 μM; $ZnSO_4$, 0.75 μM; $FeSO_4$, 0.75 μM; pH buffered at 7 with 10 mM sodium phosphate). Successive scans were carried out at the beginning of the incubation, and after 90 min, 6 h, and 24 h. The concentration of fluorescent sample (1 μM) was in the linear range of measurement of the spectrofluorometer (Perkin-Elmer LS50-B). Samples were excited at 280 nm, the excitation and emission slits being 2.5 and 10 nm, respectively. The experiment was repeated 5 times with equivalent results. The fluorescence spectra of the three fully denatured aFGF forms (in the presence urea 8 M), at the aforementioned protein concentrations, are equivalent. At the end of the incubation, the samples were centrifuged (14000*g*, 10 min, 277 K), and unspecific protein loss in the solution was estimated by addition of 8 M urea. This value (always <17% of the amount of protein at the beginning of the incubation) was not appreciably different among the three proteins.

show that aFGF mitogenic activity does not have an absolute requirement for the DNA-replication inducing activity, specific of the peptides whose sequences match that spanning residues 23−26 of aFGF.

Denaturation of aFGF$^{27-154}$, aFGF$^{23-154}$, and aFGF^{4Ala} at the Conditions of Temperature and Ionic Composition of the Mitogenesis Assay. Differences in denaturation rates between aFGF$^{27-154}$ and the wild-type protein, at the conditions of temperature and ionic composition of the medium of the mitogenic assay, were studied to find out whether such differences somehow correlate with those in their mitogenic activity. It should be taken into account that free -SH groups of aFGF oxidize very easily in the presence of traces of transition metals, with the subsequent loss of mitogenic activity of the protein (*60*). Differences in denaturation rates thus provide a reasonable estimate of the relative stability of these proteins against those agents. aFGF$^{23-154}$ was used throughout the study reported here as wild-type protein (see the introduction). Denaturation of aFGF was monitored using the fluorescence enhancement of its single Trp (*61*). Figure 3A shows that the native aFGF barely fluoresces at 350 nm, at the beginning of the experiment, and there is accumulation of fluorescent aFGF species as the incubation progresses. Denaturation of the protein structure was nearly instantaneous when heparin was omitted from the mixture. DTT at 200 μM retards the denaturation significantly, suggesting the involvement of Cys oxidation. Addition of EDTA (5 mM) to the incubation medium also greatly retarded the denaturation of the protein, consistent with the participation of transition metals in the oxidation of the -SH groups of the protein. As Figure 3B shows, aFGF$^{27-154}$ denatures under the same conditions, at a considerably slower rate. The fluorescence spectrum of native aFGF$^{23-154}$ after 24 h of incubation compared with that in the presence of 8 M urea under identical solution conditions indicated that approximately 60% of the protein denatures during this period of incubation. Equivalent measurements show that only 24% of the protein is denatured in the case of aFGF$^{27-154}$ during the same time period. The denaturation rate of aFGF^{4Ala} (Figure 3C) incubated under the same conditions closely resembled that of aFGF$^{27-154}$.

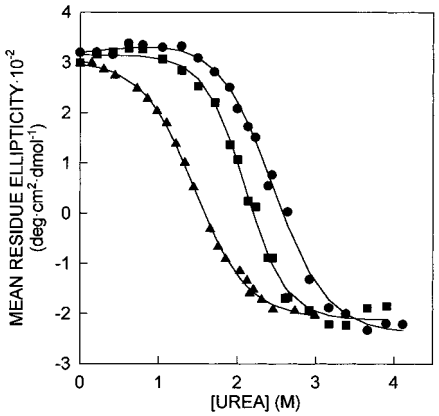

FIGURE 4: Ellipticity (227 nm) at equilibrium of aFGF$^{23-154}$ (■), aFGF$^{27-154}$ (▲), and aFGF^{4Ala} (●), at increasing urea concentrations.

Denaturation of the three aFGF forms at the conditions of temperature and ionic composition of the medium of the mitogenic assay contrasts with the $\Delta G_D^{H_2O}$ values estimated for the three proteins by urea denaturation. Denaturation profiles obtained for aFGF$^{23-154}$, aFGF$^{27-154}$, and aFGF^{4Ala} appear in Figure 4. Best fits for the data (*62*) yield $\Delta G_D^{H_2O}$ values of 4.02, 2.76, and 4.64 kcal·mol^{-1}, respectively, results which agree with previous comparative studies carried out with the two first protein forms (*37*, *41*). Comparison of these data with those of Figure 3 reveals that the relative stability of the three aFGF forms in the mitogenesis medium is not linearly related to the relative stability of their three-dimensional structure.

Three-Dimensional Structure in Solution of aFGF$^{27-154}$ and aFGF^{4Ala}. Determination of the three-dimensional structures of aFGF$^{27-154}$ and aFGF^{4Ala} was carried out on the basis of two-dimensional COSY, TOCSY, and NOESY spectra (*63*, *64*) obtained at 298 K in $H_2O/^2H_2O$ using the same procedure as those used in solving the structure of the mitogenically active aFGF$^{23-154}$ (MIHS-bound; *10*). The signal corresponding to water was eliminated from the

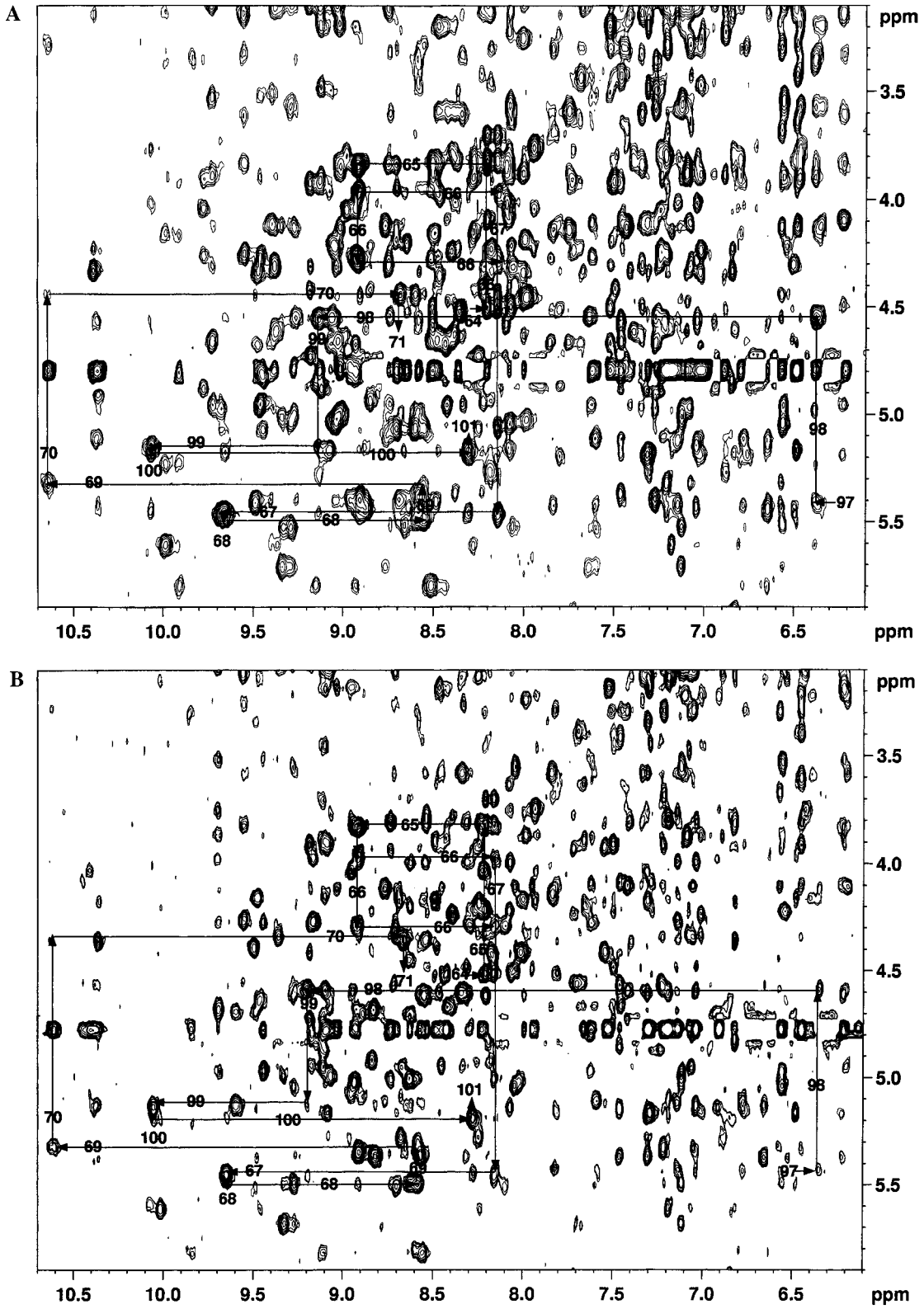

FIGURE 5: Phase-sensitive 150 mM NOESY spectrum of 1 mM aFGF^{4Ala} (A) and aFGF$^{27-154}$ (B) bound to MIHS showing the sequential assignment of segments 64−71 and 97−101. The sequential NH−C$^{\alpha}$H assignments are indicated by arrows ($H_2O/^2H_2O$, 9:1; 298 K).

NOESY spectra using the WATERGATE module (*52*), which allowed the identification of C$^{\alpha}$H proton signals with chemical shifts very close to that of water. The sequential assignment was facilitated by those previously carried out (*10*, *11*, *65*). The quality of the spectra and the sequential assignment pathway of segments 64−71 and 97−101 of aFGF^{4Ala} and aFGF$^{27-154}$ are illustrated in the fingerprint region of the NOESY spectra of Figure 5A,B, respectively. Differences in δ-values of NH-amide and C$^{\alpha}$H protons between aFGF$^{27-154}$ and aFGF$^{23-154}$, and aFGF^{4Ala} and aFGF$^{23-154}$, respectively, at each residue are plotted in Figure 6. The figure shows that differences in δ-values of NH-amide and C$^{\alpha}$H resonances are for most residues lower than 0.10 and 0.05 ppm, respectively, which indicates a high similarity

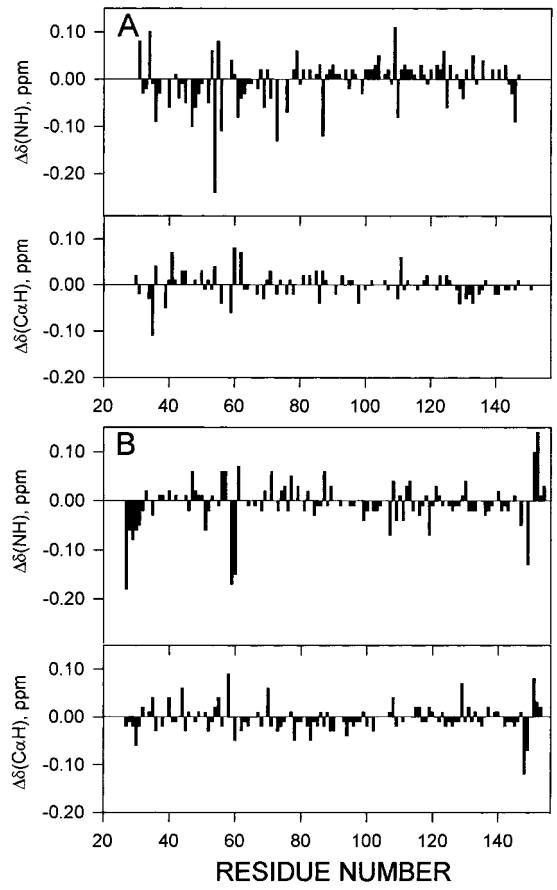

FIGURE 6: Differences in δ-values of the NH amide (upper panels) and $C^{\alpha}H$ (lower panels) protons for each residue of $aFGF^{27-154}$ (A) and $aFGF^{4Ala}$ (B) with $aFGF^{23-154}$. δ-values for $aFGF^{23-154}$ were those from Pineda-Lucena et al. (*10*). In all cases, the protein was bound to MIHS.

in the folding of the three proteins. The quality of the spectra clearly indicates that $aFGF^{27-154}$ and $aFGF^{4Ala}$ are quite stable proteins.

The three-dimensional structures of $aFGF^{27-154}$ and $aFGF^{4Ala}$ were calculated as described under Materials and Methods. The number and types of constraints derived from the analysis of phase-sensitive 150 ms NOESY spectra that were used in the calculation of the structures are summarized in Table 1. The three-dimensional structure of $aFGF^{23-154}$ bound to MIHS was also recalculated using the distance constraints of Pineda-Lucena et al. (*10*). This structure was used throughout the studies reported here in comparisons with those of $aFGF^{27-154}$ and $aFGF^{4Ala}$. A superposition of the main chains of the set of conformers obtained for $aFGF^{27-154}$ and $aFGF^{4Ala}$, respectively, appears in Figure 7A,B, and the corresponding structural statistics in Table 2. As shown in Figure 7, both proteins adopt the overall β-folding of $aFGF^{23-154}$ (*10*, *11*, *8*), in agreement with the result of the comparisons summarized in Figure 6 and the equivalent distribution of observed NOEs along the sequences of the three proteins under consideration (Figure 8, top). This fold, known as the β-trefoil motif (schematized in Figure 7C), is formed by six β-strand pairs, five of them with hairpin structure ($\beta2-\beta3$, $\beta4-\beta5$, $\beta6-\beta7$, $\beta8-\beta9$, $\beta10-\beta11$), and another one ($\beta1-\beta12$) without, although it is topologically equivalent to the other five and sometimes also referred to as the sixth hairpin (*66*). In the case of $aFGF^{27-154}$, the two first amino acids of strand $\beta1$ of $aFGF^{4Ala}$ (and of $aFGF^{23-154}$; *10*, *11*) are absent. This probably accounts for the lower number of restrictions per residue in the case of $aFGF^{27-154}$ than in $aFGF^{4Ala}$ and $aFGF^{23-154}$, at the N- and the C-terminus (Figure 8, top), an effect that probably reflects a lower stability of the $\beta1-\beta12$ pair in the former protein, and translates in the differences in definition of the structures represented in Figure 7A,B. RS1 includes residues of this pair (*9*, *54*): Tyr29, Ser31 (strand $\beta1$); Leu147, Leu149 (strand $\beta12$). In addition, the superposition of the averaged main-chain structures of Figure 7D,E shows that the end of β-strand 3 and the loop connecting it with β-strand 4 are clearly displaced in the nonmitogenic form of the protein ($aFGF^{27-154}$) with respect to the mitogenic ones ($aFGF^{23-154}$ and $aFGF^{4Ala}$). This region, which in the three-dimensional structure of these proteins is close to the $\beta1-\beta12$ hairpin, also participates in RS1 (Arg49, Arg51; *9*, *65*). Differences in the relative position of this region with respect to the rest of the structure between the nonmitogenic $aFGF^{27-154}$ and the mitogenic $aFGF^{4Ala}$ can also be appreciated in Figure 7A,B. This figure also shows that this is a reasonably well-defined region of the structure in both polypeptides. The different position of this region in the two proteins is the consequence of a quite large number of NOE cross-correlations with small to medium different intensities. A complete list of the experimental constraints is deposited in the PDB. Differences in orientation at the end of β-strand 3 and the loop connecting it with β-strand 4, between the nonmitogenic $aFGF^{27-154}$ and the mitogenic forms, also appear reflected in the plot of the backbone RMS deviations among the different structures (Figure 8, bottom), which shows a major peak at the residues corresponding to this region. In addition, the plot presents a further major peak, albeit smaller than the one corresponding to residues 48−53, at the region of residues 104−108. This region, that corresponds to the end and beginning of β-strands 8 and 9, respectively, and the loop connecting them, includes residues Glu104, Ans106, and Tyr108, which also seem to participate in RS1, according to site mutagenesis studies (*9*; Redondo-Horcajo, M., unpublished observations). Differences in the relative position of this region with respect to the rest of the structure between the nonmitogenic $aFGF^{27-154}$ and the mitogenic forms of the protein can also be appreciated in Figure 7D,E.

Table 1: Number and Types of NOE Restraints Used in Calculation of Structures

	$aFGF^{27-154}$ [distance (Å)]				$aFGF^{4Ala}$ [distance (Å)]			
type	<3.5	3.5−4.5	≥4.5	total	<3.5	3.5−4.5	≥4.5	total
intraresidual ($\|i-j\|=0$)	177	132	127	436	143	37	30	210
sequential ($\|i-j\|=1$)	102	63	176	341	179	72	137	388
medium-range ($2 \le \|i-j\| \le 5$)	11	39	116	166	30	21	91	142
long-range ($\|i-j\|>5$)	35	55	455	545	39	39	454	590
all				1488				1330

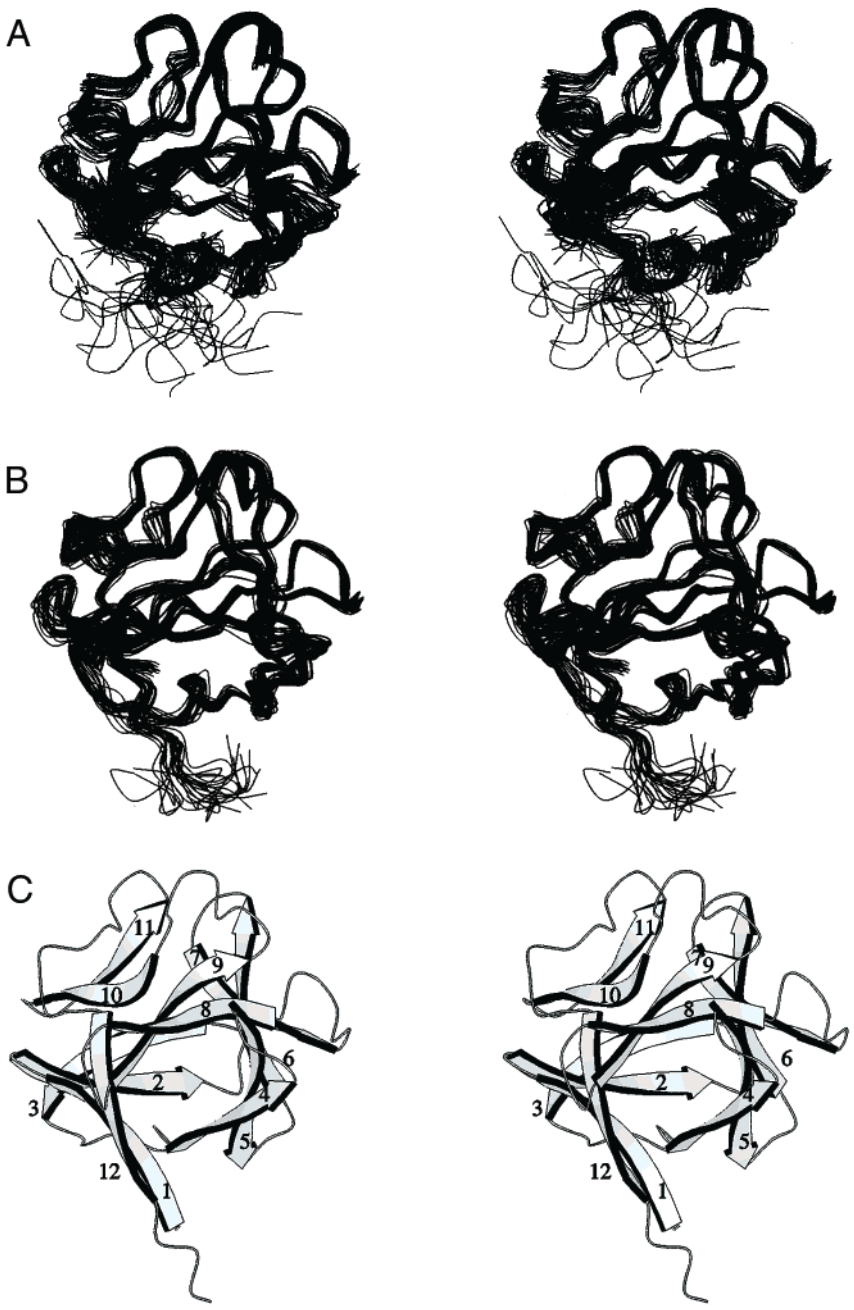

Vasodilatory Activity and Structure of RS2. Site-directed mutagenesis studies carried out by Springer et al. (*9*), with bFGF, indicated that Lys115, Tyr116, and Trp121 (based on the aFGF numbering scheme) belong to RS2, a second site of interaction with the cell membrane receptors, which is of less importance for mitogenesis than RS1. Both Lys115 and Trp121 are conserved in aFGF, while Tyr116 is conservatively substituted by His (*33*). Trp121 and Lys115 are at the beginning of β-strand 10 and the loop connecting β-strands 9 and 10, respectively (*10*). In the case of bFGF, this region includes five residues, while in the case of aFGF the corresponding region is comprised of seven residues. By substituting the longer loop region from aFGF into bFGF, Seddon et al. (*67*) have shown that RS2 is a critical determinant for the selective recognition of different cell-surface FGF receptors derived by alternative splicing of the transcripts of the four different genes coding for such receptors (*6*). As the vasodilatory, neuromodulatory, and cardio- and neuroprotective activities of aFGF$^{27-154}$ are equivalent to those of the wild-type protein (*42*−*45*), the differences between the structures of the two proteins at the level of RS1 (see above) suggest that RS2 should be a key domain for such activities. Figure 9A shows the superposition of the relative three-dimensional position of the residues of RS2 of the 24 conformers resulting from calculation of the structure of aFGF$^{27-154}$. As the figure shows, the side chains of Lys115, His116, and Trp121 are well-defined (RMSD 0.63, 0.37, and 0.34 Å, respectively), the planes of the two aromatic rings defining an average dihedral angle of −46°, and the Lys115 side chain, approximately at the center of a half-ring of negative charges belonging to the side chains of Asp82, Glu95, Glu96, and Glu118, pointing its ϵ-amino group toward the δ-carboxyl group of Glu118. A similar geometry is observed in the three-dimensional structures of the longer forms of aFGF calculated either by NMR or by X-ray diffraction (*8*, *10*, *11*, *29*, *68*). However, in the case

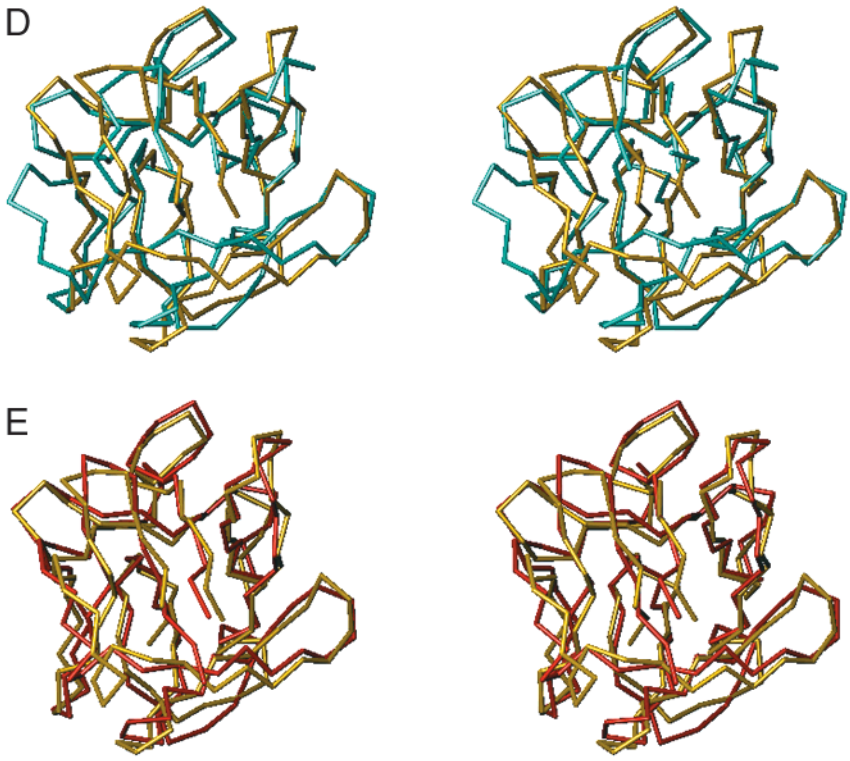

FIGURE 7: Stereoview of the best-fit backbone superposition of the 24 structures derived from the restrained molecular dynamics calculations of aFGF$^{27-154}$ (A) and aFGF^{4Ala} (B), respectively, of the schematic representation of the β-trefoil topology (C), and of the averaged structures of aFGF$^{27-154}$ (D) and aFGF^{4Ala} (E) superimposed to that of aFGF$^{23-154}$ (recalculated from the distance constraints of ref *10*). In (A) and (B), the C-terminus is at the bottom of the figure and the loop connecting β-strands 3 and 4, just above it. The N-terminus of β-strand 1 in (C) corresponds to Lys26 and the C-terminus to Asp154. In (D) and (E), only the main chains of residues 25 (28 in aFGF$^{27-154}$) to 150 were averaged, which correspond to the beginning of β-strand 1 in unmodified aFGFs (*10*, *29*) and to the end of β-strand 12, respectively. Light blue, aFGF$^{27-154}$; red, aFGF^{4Ala}; yellow, aFGF$^{23-154}$. In (D) and (E), the loop connecting β-strands 3 and 4 of aFGF$^{27-154}$ appears at the left bottom corner of the figure, that connecting β-strands 8 and 9 at the top right and the C-terminus at the center.

Table 2: Structural Statistics: Residual Constraint Violations

range (Å)	av no. of distance constraint violations	
	aFGF$^{27-154}$	aFGF^{4Ala}
0.00−0.25	159.2	168.9
0.25−0.50	101.1	120.2
0.50−0.75	24.5	38.4
0.75−1.00	7.1	4.9
>1.00	0.7	0.5
max violation (Å)	1.4	1.1
av sum of violations (Å)	82.7	93.2
pairwise RMSDs		
backbone (Å)	0.94 (30...148)	0.90 (27...150)
heavy atoms (Å)	1.69	1.65
total energy (kJ mol^{-1})		
average	−6185	−7153
range	−7127 to −5129	−7884 to −5920
Lennard−Jones energy (kJ mol^{-1})		
average	−4661	−4993
range	−4545 to −4767	−4908 to −5084
NOE term (kJ mol^{-1})		
average	681	753
range	574−760	685−817

of aFGF^{4Ala}, the conformation of RS2 appears considerably altered. As Figure 9B shows, His116 is displaced from the relative position it occupies in Figure 9A by Lys115, whose ϵ-amino group points toward Asp82 instead of Glu118, a shift that is accompanied by an increase in the structural definition of the former residue and a decrease of the latter one when compared with those in aFGF$^{27-154}$, as reflected by the RMSD of the superimposed side chains (1.92 Å for Asp82 and 1.6 Å for Glu118 in aFGF$^{27-154}$; 1.64 Å for Asp82 and 2.69 Å for Glu118 in aFGF^{4Ala}). Repositioning of Lys115 is accompanied by a decrease of its definition (RMSD 0.63 and 1.81 Å in Figures 9A and 9B, respectively). Displacement of His116 in aFGF^{4Ala} also causes a considerable decrease of its definition (RMSD, 1.5 Å) in comparison with the aFGF$^{27-154}$ case and modifies the average dihedral angle of the plane of its ring relative to that of Trp121 (−83°). Taken together, these observations suggest that RS2 of aFGF^{4Ala} should be poorly recognized and, consequently, activities such as the vasodilatory one present at normal levels in aFGF$^{27-154}$ should become affected in aFGF^{4Ala}. Effectively, as exemplified in Figure 10, the decrease in blood pressure following vasodilation was consistently smaller in animals treated with aFGF^{4Ala} than in those receiving equivalent subsaturating doses of aFGF$^{23-154}$ (*42*).

Stability at Mitogenic Assay Conditions and Accessibility of Cys131 to the Solvent. Enhancement by DTT of the stability of aFGF$^{23-154}$, incubated in conditions equivalent to those in the mitogenic assays, suggests an important role for free Cys in its denaturation. A visual examination of the surface of the protein using the van der Waals radii for the representation of all the heavy atoms shows that Cys30 and Cys131 are more solvent-exposed in aFGF$^{23-154}$ (Figure 11A) than in aFGF$^{27-154}$ (Figure 11B), which seem to provide a reasonable explanation for the differences observed between their respective denaturation rates (Figure 3). However, the special sensitivity to trypsin digestion of aFGF$^{27-154}$ reported by Luo et al. (*41*) suggests that the differences in solvent

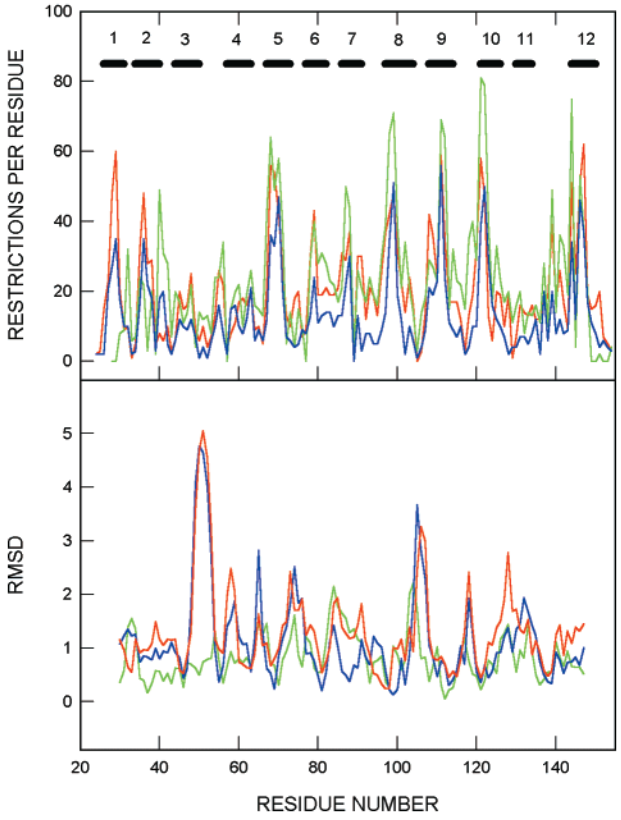

FIGURE 8: Top: number of restrictions per residue along the sequence of aFGF$^{27-154}$ (green), aFGF$^{23-154}$ (blue), and aFGF^{4Ala} (red). Bottom: backbone RMSD at each residue among the best-fit main-chain superimpositions of the mitogenic forms of the protein (aFGF$^{23-154}$ and aFGF^{4Ala}, green) and of each one of them (aFGF$^{23-154}$, blue; aFGF^{4Ala}, red) with the backbone of aFGF$^{27-154}$. Data of aFGF$^{23-154}$ are from ref *10*. The span of the 12 β-strands of the β-trefoil structure appears at the top of the figure.

accessibility could be less dramatic than suggested by the structures depicted in Figure 11, since sensitivity to proteases directly correlates with flexibility in the three-dimensional structure (*30*−*32*). A shielding of Cys30 and Cys131 was also observed in aFGF^{4Ala} as in the case of aFGF$^{27-154}$ (not shown).

DISCUSSION

Since the engineering of the nonmitogenic aFGF$^{27-154}$ was first reported (*34*), considerable attention has been paid to this polypeptide as a tool for the elucidation of the structural basis of FGF biological activities, and for its potential therapeutic applications (see the introduction). Our studies suggest that the lack of mitogenic activity of this polypeptide derives from the alteration of the RS1 structure. Moreover, our results also suggest a predominant role of RS2 in mediating the vasodilatory activity of FGF. This probably extends to neuromodulatory and ischemia protecting activities, as they seem equivalent in aFGF$^{27-154}$ and the wild-type protein.

Differences in specific mitogenic activity between aFGF$^{27-154}$ and aFGF$^{23-154}$ show the relevance of the sequence Lys-Lys-Pro-Lys in aFGF-driven mitogenesis. Although it has been shown that cell membrane-permeable peptides containing the Asn-Tyr-Lys-Lys-Pro-Lys sequence can stimulate DNA synthesis (*39*, *40*), the specific mitogenic activities measured for aFGF^{4Ala} rule out the stretch Lys-Lys-Pro-Lys as an essential mediator of aFGF mitogenic activity. These results also rule out the proposed role of this sequence stretch as a signal sequence for the translocation of the growth factor into the nucleus that is required in FGF-driven mitogenesis (*34*, *37*, *21*). Our results rather point toward a mere bulk function of these amino acids in the overall structure of the protein. Luo et al. (*41*) have suggested, on the basis of studies on denaturation rates at 85 °C and resistance to trypsin digestion, that the differences in mitogenic activity between the wild-type protein and aFGF$^{27-154}$ arise from the lower stability of the latter. Nevertheless, it is obvious that the mitogenesis assays can have specific effects on the stability of FGF, different from those used by Luo et al. (*41*) in their protease and thermal denaturation tests. Thus, different ions in the media used for the mitogenesis assays may catalyze a fast oxidation of the free -SH of aFGF, causing its inactivation (*60*). Here we have shown that under the incubation conditions which emulate the mitogenesis medium, the wild-type protein is less stable than aFGF$^{27-154}$ or aFGF^{4Ala}, and that the free sulfhydryl groups of the protein and metals that can be chelated by EDTA are key players in this denaturation. Moreover, structural results shown here point toward the more solvent-exposed Cys131 as the main one responsible for the instability of aFGF under the mitogenesis assay conditions, in agreement with previous site-directed mutagenesis of Cys131 (*60*, *69*). The high dispersion and narrow signals of the ^{1}H NMR spectra observed (Figure 5), typical for well-defined native structures, could not have been obtained for an unstable protein. Moreover, translocation to the cytoplasm observed in other studies does not seem compatible with a rapid denaturation of the protein during the mitogenesis assay incubation (*20*, *38*).

That a certain alteration of the structure of RS1 could be compatible with the maintenance at normal levels of the specific activity of some of the biological activities of FGF is an observation parallel to those of Isacchi et al. (*70*) on the selective elimination of the bFGF capacity of stimulating plasminogen activator production in endothelial cells by deletion of amino acids 28−32, which in the three-dimensional structure corresponds to the Lys-Lys-Pro-Lys stretch in aFGF. Altogether, these results point toward the possible existence of several signaling FGF−cell receptor assemblages. Binding of FGF to its cell membrane receptor as a complex event, able to elicit different signals according to the specific characteristics of the formed complex, is also suggested by the studies of Kudla et al. (*71*). Elaboration of a detailed model of the activation of cell membrane FGF receptors should probably await the results of further high-resolution structural studies. Up to now, two opposing models for the formation of the FGF−cell receptor complex have been proposed. In the first (*72*), the authors propose that activation of FGF receptors involves the cross-phosphorylation of two receptor units brought close enough by their respective binding to two FGF units already cross-linked by a heparin fragment of adequate length. In the second model (*73*), it was proposed, on the basis of isothermal titration calorimetry and sedimentation equilibrium studies of the reciprocal interaction of heparin, FGF, and the extracellular moiety of the cell receptor, that they assemble as a 1:1:2 complex, with the participation of RS1 and RS2, in a highly cooperative kinetic process with many short-lived intermedi-

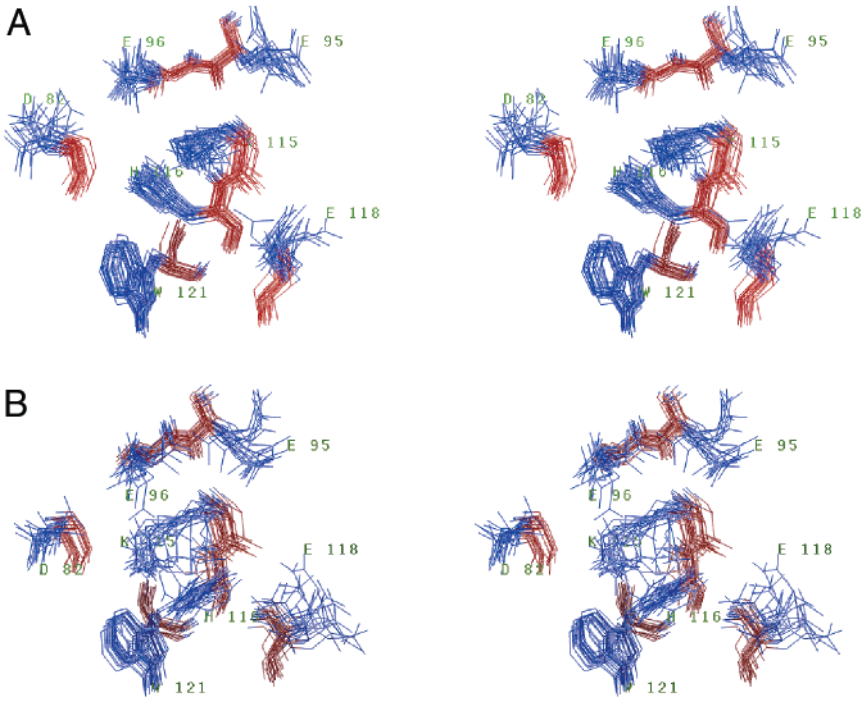

FIGURE 9: Relative position of the residues of RS2 (red, backbone; blue, side chain) in the best-fit superpositions of the 24 conformers resulting from the restrained molecular dynamics calculations for aFGF$^{27-154}$ (A) and aFGF^{4Ala} (B).

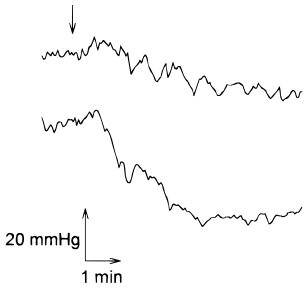

FIGURE 10: Effect of intravenous 2 μg injections of aFGF^{4Ala} (upper trace) and aFGF$^{23-154}$ (lower trace) on the mean arterial blood pressure of anesthetized rats. Blood pressure was measured as described in Cuevas et al. (*42*).

ates. It would not be surprising if the binding of FGF with modified RS1 or RS2 causes in each case an alteration in the level of certain of those intermediates, with the subsequent modification of the spectrum of receptor tyrosine autophosphorylation (*14*) and the set of intracellular signals mediating the normal cell answer to the FGF challenge. Actually, Dell'Era et al. (*74*) have recently shown that different autophosphorylated tyrosines of the FGF receptor signal plasminogen activator induction and mitogenesis. Recent characterization by Hsu et al. (*75*) of ligand−receptor complexes of heparin, FGF-7, and the extracellular moiety of its receptor, which is also recognized by aFGF, by size exclusion chromatography, light scattering, N-terminal protein sequencing, and sedimentation velocity also suggests that they assemble as a 1:1:2 complex. Recently, the crystal structure of the complex bFGF and part of the extracellular moiety of the FGF receptor in the absence of heparin has been reported (*76*). These data show that two bFGF−FGF receptor complexes form a 2-fold symmetric dimer. It is obvious that these results do not exclude that other sorts of complexes could assemble. Finally, it cannot be ruled out that the alterations of the RS1 domain of aFGF$^{27-154}$ prevent it from being able to form the exact kind of complex with

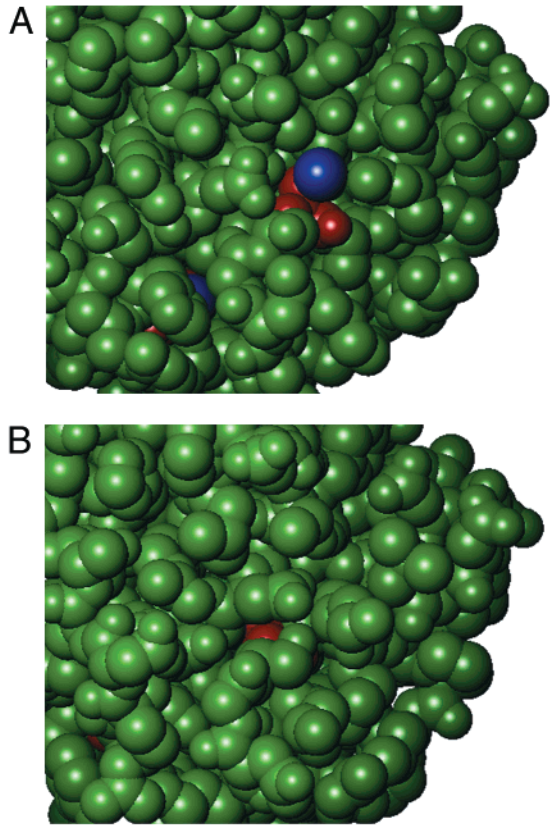

FIGURE 11: CPK solid representation of the face at which the -SH groups (blue color) of both Cys30 and Cys131 (red color) become accessible to the solvent in the energy-minimized (*58*) average structure of aFGF$^{23-154}$ (A). The representation of aFGF$^{27-154}$ in the same orientation is shown in (B). The highest exposed -SH groups correspond to Cys131. The structure of aFGF$^{23-154}$ was recalculated from the distance constraints of ref *10*.

the cell membrane receptor that triggers the process of translocation of FGFs to the nucleus. Nevertheless, the

elaboration of a reasonable model to account for the inability of aFGF$^{27-154}$ to be exported to the nucleus must wait until details of the mechanism responsible for this process become available.

The effect of the substitution of Lys-Lys-Pro-Lys at positions 23−26 by a four Ala sequence on the second receptor recognition site was unpredictable. Nevertheless, the folding of FGFs is probably very cooperative and its three-dimensional structure very malleable as it is mainly maintained by a hydrophobic core to which all the strands contribute without participation of interstrand covalent bonds. Thus, slight modifications in one precise location of the protein can affect quite significantly regions at the opposite side of the structure. Such was the case for *myo*-inositol hexasulfate binding. Pineda-Lucena et al. (*10*) have reported that the attachment of this compound to its binding site, constituted by residues of strands 10 and 11 and the loop connecting β-strands 11 and 12, induces specific conformational changes in the region of β-strands 1−5, located at a distal position.

It cannot be totally ruled out, on the basis of the data reported here, that RS1 plays a secondary role in FGF vasodilatory activity, as its structure is only partially modified in aFGF$^{27-154}$. At the same time, structural changes in RS2 could also be the cause of the lower specific activity of aFGF^{4Ala} with respect to aFGF$^{23-154}$ in the mitogenesis assays (Figure 2). Thus, the structural analyses reported here of aFGF$^{27-154}$ and aFGF^{4Ala} may only imply RS1 and RS2 domains to be merely predominant players in the mitogenic and vasodilatory activities of FGFs, respectively. Actually, Springer et al. suggested when RS2 was first described (*9*) that it is involved in the mitogenic activity of the protein at a less important rate than RS1. Our results also support that those domains can be modified independently. This suggests that the generation of aFGF forms in which either the mitogenic or the vasodilatory, neuromodulatory, and protective activities have been selectively eliminated is a wide-open possibility. The possibility of generating such forms is of obvious interest for the pharmacological developments of aFGF, as it may allow fine-tuning in its therapeutic applications. In addition, it seems feasible to develop structural analogues of RS2, given its relative structural simplicity. The synthesis of such structural analogues may constitute a novel route for generating new compounds in treating a wide assortment of human pathologies, given the relevance of RS2 for the vasodilatory activity of aFGF and, probably, for its neuromodulatory and cardio- and neuroprotective activities.

ACKNOWLEDGMENT

We thank S. Padmanabhan for critical reading of the manuscript and M. Zazo, C. López, A. Gómez, and L. de la Vega for excellent technical assistance.

SUPPORTING INFORMATION AVAILABLE

Resonance assignments (9 pages). This material is available free of charge via the Internet at http://pubs.acs.org.

REFERENCES

1. Nishimura, T., Utsunomiya, Y., Hoshikawa, M., Ohuchi, H., and Itoh, N. (1999) *Biochim. Biophys. Acta 1444*, 148−151.
2. Coulier, F., Pontarotti, P., Roubin, R., Hartung, H., Goldfarb, M., and Birnbaum, D. (1997) *J. Mol. Evol. 44*, 43−56.
3. Thomas, K. A., and Giménez-Gallego G. (1986) *Trends Biochem. Sci. 11*, 1−4.
4. Baird, A., and Böhlen, P. (1990) *Handb. Exp. Pharmacol. 95*, 369−418.
5. Giménez-Gallego, G., and Cuevas, P. (1994) *Neurol. Res. 16*, 313−316.
6. Jaye, M., Schlessinger, J., and Dionne, C. A. (1992) *Biochim. Biophys. Acta 1135*, 185−199.
7. Baird, A., Schubert, D., Ling, N., and Guillemin, R. (1988) *Proc. Natl. Acad. Sci. U.S.A. 85*, 2324−2328.
8. Zhu, X., Komiya, H., Chirino, A., Faham, S., Fox, G. M., Arakawa, T., Hsu, B. T., and Rees, D. C. (1991) *Science 251*, 90−93.
9. Springer, B. A., Pantoliano, M. W., Barbera, F. A., Gunyuzlu, P. L., Thompson, L. D., Herblin, W. F., Rosenfeld, S. A., and Book, G. W. (1994) *J. Biol. Chem. 269*, 26879−26884.
10. Pineda-Lucena, A., Jiménez, M. A., Nieto, J. L., Santoro, J., Rico, M., and Giménez-Gallego, G. (1994) *J. Mol. Biol. 242*, 81−98.
11. Pineda-Lucena, A., Jiménez, M. A., Lozano, R. M., Nieto, J. L., Santoro, J., Rico, M., and Giménez-Gallego, G. (1996) *J. Mol. Biol. 264*, 162−178.
12. Arakawa, T., Holst, P., Narhi, L. O., Philo, J. S., Wen, J., Prestrelski, S. J., Zhu, X. T., Rees, D. C., and Fox, G. M. (1995) *J. Protein Chem. 5*, 263−274.
13. Burgess, W. H., and Maciag, T. (1989) *Annu. Rev. Biochem. 58*, 575−606.
14. Mohammadi, M., Dikic, I., Sorokin, A., Burgess, W. H., Jaye, M., and Schlessinger, J. (1996) *Mol. Cell. Biol. 16*, 977−989.
15. Huang, J. T., Mohammadi, M., Rodrigues, G. A., and Schlessinger, J. (1995) *J. Biol. Chem. 270*, 5065−5072.
16. Pandiella, A., Magni, M., and Meldolesi, J. (1989) *Biochem. Biophys. Res. Commun. 163*, 1325−1331.
17. Gay, C. G., and Winkles, J. A. (1991) *Proc. Natl. Acad. Sci. U.S.A. 88*, 296−300.
18. Wiecha, J., Reineker, K., Reitmayer, M., Voisard, R., Hannekum, A., Mattfeldt, T., Waltenberger, J., and Hombach, V. (1998) *Growth Horm. IGF Res. 8*, 175−181.
19. Wiecha, J., Münz, B., Wu, Y., Noll, T., Tillmanns, H., and Waldecker, B. (1998) *J. Vasc. Res. 35*, 363−371.
20. Wiedlocha, A., Falnes, P. O., Rapak, A., Munoz, R., Klingenberg, O., and Olsnes, S. (1996) *Mol. Cell. Biol. 16*, 270−280.
21. Mehta, V. B., Connors, L., Wang, H.-C. R., and Chiu, I.-M. (1998) *J. Biol. Chem. 273*, 4197−4205.
22. Thomas, K. A., Rios-Candelore, M., and Fitzpatrick, S. (1984) *Proc. Natl. Acad. Sci. U.S.A. 81*, 357−361.
23. Thomas, K. A., Rios-Candelore, M., Giménez-Gallego, G., DiSalvo, J., Bennett, C., Rodkey, J., and Fitzpatrick, S. (1985) *Proc. Natl. Acd. Sci. U.S.A. 82*, 6409−6413.
24. Giménez-Gallego, G., Conn, G., Hatcher, V. B., and Thomas, K. A. (1986) *Biochem. Biophys. Res. Commun. 138*, 611−617.
25. Burgess, W. H., Mehlman, T., Friesel, R., Johnson, W. V., and Maciag, T. (1985) *J. Biol. Chem. 260*, 11389−11392.
26. Burgess, W. H., Mehlman, T., Marshak, D. R., Fraser, B. A., and Maciag, T. (1986) *Proc. Natl. Acad. Sci. U.S.A. 83*, 7216−7220.
27. Jaye, M., Howk, R., Burgess, W., Ricca, G. A., Chiu, I.-M., Ravera, M. W., O'Brien, S. J., Modi, W. S., Maciag, T., and Drohan, W. N. (1986) *Science 233*, 541−545.
28. Ueno, N., Baird, A., Esch, F., Ling, N., and Guillemin, R. (1986) *Biochem. Biophys. Res. Commun. 138*, 580−588.
29. Romero, A., Pineda-Lucena, A., and Giménez-Gallego, G. (1996) *Eur. J. Biochem. 241*, 453−461.
30. Fontana, A., Fassina, G., Vita, C., Dalzoppo, D., Moreno, Z., and Zambonin, M. (1986) *Biochemistry, 25*, 1847−1851.
31. Signor, G., Vita, C., Fontana, A., Frigerio, F., Bolognesi, M., Toma, S., Gianna, R., De Gregoriis, E., and Grandi, G. (1990) *Eur. J. Biochem. 189*, 221−227.

32. Polverino de Laureto, P., De Filippis, V., Di Bello, M., Zambonin, M., and Fontana, A. (1995) *Biochemistry 34*, 12596−12604.
33. Dayhoff, M. O., Schwartz, R. M., and Orcutt, B. C. (1978) in *Atlas of Protein Sequence and Structure* (Dayhoff, M. O., Ed.) Vol. 5, Suppl. 3, pp 345−358, National Biomedical Research Foundation, Washington, DC.
34. Imamura, T., Engleka, K., Zhan, X., Tokita, Y., Forough, R., Roeder, D., Jackson, A., Maier, J. A. M., Hla, T., and Maciag, T. (1990) *Science 249*, 1567−1571.
35. Dang, C. V., and Lee, W. M. (1989) *J. Biol. Chem. 264*, 18019−18023.
36. Silver, P., and Goodson, H. (1989) *Crit. Rev. Biochem. Mol. Biol. 24*, 419−435.
37. Zhan, X., Hu, X. G., Friedman, S., and Maciag, T. (1992) *Biochem. Biophys. Res. Commun. 188*, 982−991.
38. Wiedlocha, A., Falnes, P. O., Madshus, I. H., Sandvig, K., and Olsnes, S. (1994) *Cell 76*, 1039−1051.
39. Lin, Y. Z., Yao, S. Y., and Hawiger, J. (1996) *J. Biol. Chem. 271*, 5305−5308.
40. Komi, A., Suzuki, M., and Imamura, T. (1998) *Exp. Cell. Res. 243*, 408−414.
41. Luo, Y., Gabriel, J. L., Wang, F., Zhan, X., Maciag, T., Kan, M., and McKeehan, W. L. (1996) *J. Biol. Chem. 271*, 26876−26883.
42. Cuevas, P. F., Carceller, S., Ortega, M., Zazo, I., Nieto, and Giménez-Gallego, G. (1991) *Science 254*, 1208−1210.
43. Cuevas, P., Carceller, F., Lozano, R. M., Zazo, M., and Giménez-Gallego, G. (1997) *Growth Factors 15*, 29−40.
44. Cuevas, P., Carceller, F., Muñoz-Willery, I., and Giménez-Gallego, G. (1998) *Surg. Neurol. 49*, 77−84.
45. Guaza, C., Garcia-Andres, C., Sandi, C., Munoz-Willery, I., Cuevas, P., and Gimenez-Gallego, G. (1996) *Neuroscience 75*, 805−813.
46. Zazo, M., Lozano, R. M., Ortega, S., Varela, J., Díaz-Orejas, R., Ramírez, J. M., and Giménez-Gallego, G. (1992) *Gene 113*, 231−238.
47. Masui, Y., Coleman, J., and Inouye, M. (1983) in *Experimental manipulation of gene expression* (Inouye, M., Ed.) pp 15−32, Academic Press, New York.
48. Sanz, J. M., and Gimenez-Gallego, G. (1997) *Eur. J. Biochem. 246*, 328−35.
49. Pace, C. N. (1986) *Methods Enzymol. 131*, 266−280.
50. Matouschek, A., Serrano, L., and Fersht, A. R. (1992) *J. Mol. Biol. 224*, 819−35.
51. Marion, D., and Wüthrich, K. (1983) *Biochem. Biophys. Res. Commun. 113*, 967−974.
52. Piotto, M., Saudek, V., and Sklenar, V. (1992) *J. Biomol. NMR 6*, 661−665.
53. Aue, W. P., Bartholdi, E., and Ernst, R. R. (1976) *J. Chem. Phys. 64*, 2229−2246.
54. Kumar, A., Ernst, R. R., and Wüthrich, K. (1980) *Biochem. Biophys. Res. Commun. 95*, 1−6.
55. Bax, A., and Davies, D. (1985) *J. Magn. Reson. 65*, 355−360.
56. Bartels, C., Xia, T., Billeter, M., Günter, P., and Wüthrich, K. (1995) *J. Biomol. NMR 6*, 1−10.
57. Güntert, P., Braun, W., and Wüthrich, K. (1991) *J. Mol. Biol. 217*, 517−530.
58. van Gunsteren, W. F., and Berendsen, H. J. C. (1987) *Groningen molecular simulation* (GROMOS) *Library manual*, Biomos, Groningen, The Netherlands.
59. Ortega, S., García, J. L., Zazo, M., Varela, J., Muñoz-Willery, I., Cuevas, P., and Giménez-Gallego, G. (1992) *Bio/Technology 10*, 795−798.
60. Linemeyer, D. L., Menke, J. G., Kelly, L. J., DiSalvo, J., Soderman, D., Schaeffer, M.-T., Ortega, S., Giménez-Gallego, G., and Thomas, K. A. (1990) *Growth Factors 3*, 287−296.
61. Copeland, R. A., Hanlee, J., Halfpenny, A. J., Williams, R. W., Thomson, K. C., Herber, W. K., Thomas, K. A., Bruner, M. W. Ryan, J. A., Marquis-Omer, D., Sanyal, G. Sitren, R. D., Yamazaki, S., and Middaugh R. (1991) *Arch. Biochem. Biophys. 289*, 53−61.
62. Santoro, M. M., and Bolen, D. W. (1988) *Biochemistry 27*, 8063−8068.
63. Wütrich, K., Billeter, M., and Braun, W. (1984) *J. Mol. Biol. 180*, 715−740.
64. Wüthrich, K. (1986) *NMR of proteins and nucleic acids*, J. Wiley & Sons, New York.
65. Lozano, R. M., Jimenez, M., Santoro, J., Rico, M., and Gimenez-Gallego, G. (1998) *J. Mol. Biol. 281*, 899−915.
66. Murzin, A. G., Lesk, A. M., and Chothia, C. (1992) *J. Mol. Biol. 233*, 531−543.
67. Seddon, A. P., Aviezer, D., Li, L. Y., Bohlen, P., and Yayon, A. (1995) *Biochemistry 34*, 731−736.
68. Blaber, M., DiSalvo, J., and Thomas, K. A. (1996) *Biochemistry 35*, 2086−2094.
69. Ortega, S., Schaeffer, M.-T., Soderman, D., DiSalvo, J., Linemeyer, D. L., Giménez-Gallego, G., and Thomas, K. A. (1991) *J. Biol. Chem. 266*, 5842−5846.
70. Isacchi, A., Statuto, M., Chiesa, R., Bergonzoni, L., Rusnati, M., Sarmientos, P., Ragnotti, G., and Presta, M. G. (1991) *Proc. Natl. Acad. Sci. U.S.A. 88*, 2628−2632.
71. Kudla, A. J., Jones, N. C., Rosenthal, R. S., Arthur, K., Clase, K. L., and Olwin, B. B. (1998) *J. Cell Biol. 142*, 241−250.
72. Spivak-Kroizman, T., Lemmon, M. A., Dikic, I., Ladbury, J. E., Pinchsi, D., Huang, J., Jaye, M., Crumley, G., Schlessinger, J., and Lax, I. (1994) *Cell 79*, 1015−1024.
73. Pantoliano, M. W., Horlick, R. A., Springer, B. A., Van Dyk, D. E., Tobery, T., Wetmore, D. R., Lear, J. D., Nahapetian, A. T., Bradley, J. D., and Sisk, W. P. (1994) *Biochemistry 33*, 10229−10248.
74. Dell'Era, P., Mohammadi, M., and Presta, M. (1999) *Mol. Biol. Cell 10*, 23−33.
75. Hsu, Y. R., Nybo, R., Sullivan, J. K., Costigan, V., Spahr, C. S., Wong, C., Jones, M., Pentzer, A. G., Crouse, J. A., Pacifici, R. E., Lu, H. S., Morris, C. F., and Philo, J. S. (1999) *Biochemistry 38*, 2523−2534.
76. Plotnikov, A. N., Schlessinger, J., Hubbard, S. R., and Mohammadi, M. (1999) *Cell 98*, 641−650.

BI992544N